Supporting Information

Extraordinary Cycling Performance of High-Voltage Spinel $LiNi_{0.5}Mn_{1.5}O_4$ Materials Enabled by Interfacial Engineering via Molecule Self-Assembly

Chao Zhang[a], Jing-Zhe Wan[a], Liang Gao[a], Zhi-Peng Cai[a], Chao Ma[b], Kai-Xue Wang[a] and Jie-Sheng Chen[a]**

[a]*School of Chemistry and Chemical Engineering, Shanghai Jiao Tong University, Shanghai, P. R. China*

[b]*College of Smart Energy, Shanghai Jiao Tong University, Shanghai, P. R. China*

**Correspondence: Kai-Xue Wang, Jie-Sheng Chen*

E-mail: k.wang@sjtu.edu.cn, chemcj@sjtu.edu.cn

Table S1 Nyquist plots fitting data for LNMO and LNMO-DA

	LNMO Fresh	LNMO After 500 cycles	LNMO-DA Fresh	LNMO-DA After 500 cycles
*R*s （Ω）	2.56	3.487	2.68	3.11
*R*ct （Ω）	132.1	81.06	131.6	15.18

DA: decanoic acid

The X-ray Photoelectron Spectroscopy (XPS) analysis has been incorporated into our experimental procedures. However, it was observed that the LNMO-DA material, which contains a mere increment of 0.2 wt% of DA relative to the LNMO material, exhibits no discernible alterations in the Ni 2p, Mn 2p, and C1s spectra before cycling (Fig. S1a-c).

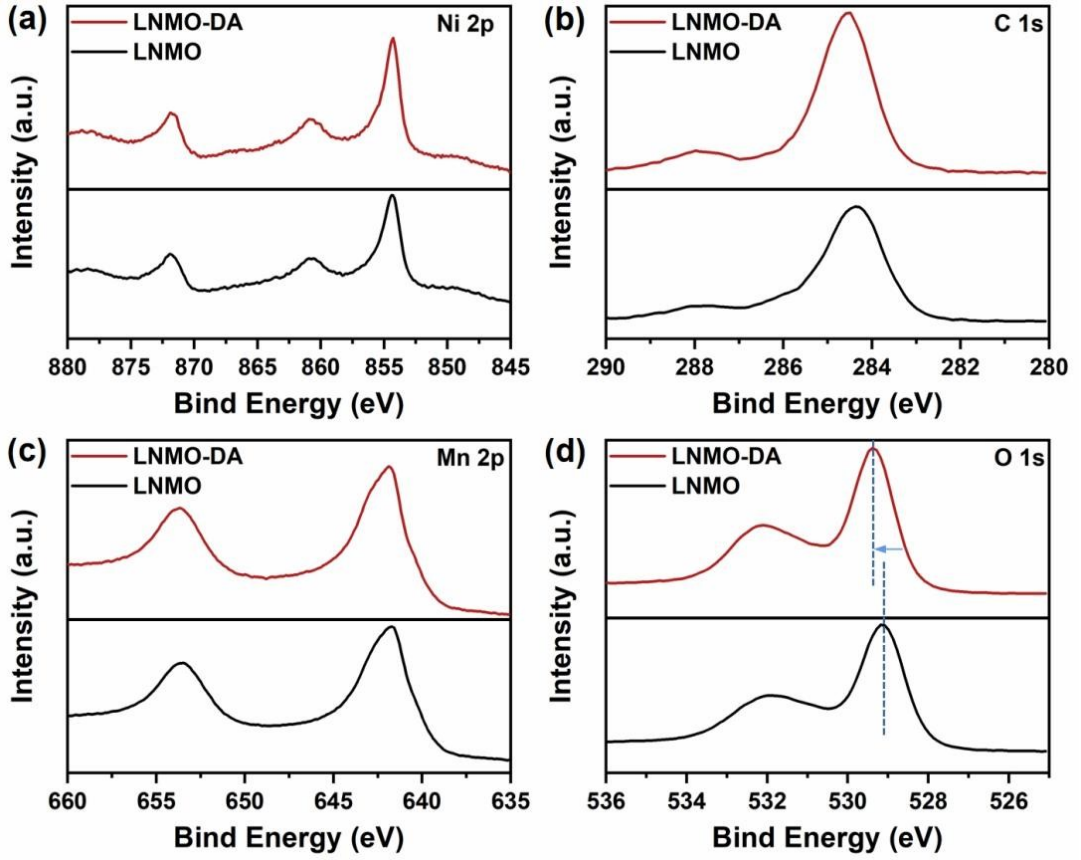

Fig. S1 (a) Ni 2p,(b) C1s,(c) Mn 2p and (d) O1s Spectra of LNMO and LNMO-DA.

Thermogravimetric analysis of LNMO and LNMO-DA materials. The actual weight of DA coating on the LNMO was revealed by the thermogravimetric analysis. As shown in Figures S2, the surface DA started to decompose at about 100 °C. According to the thermogravimetric results, the mass of the DA monolayer on the LNMO surface is approximately 0.2%.

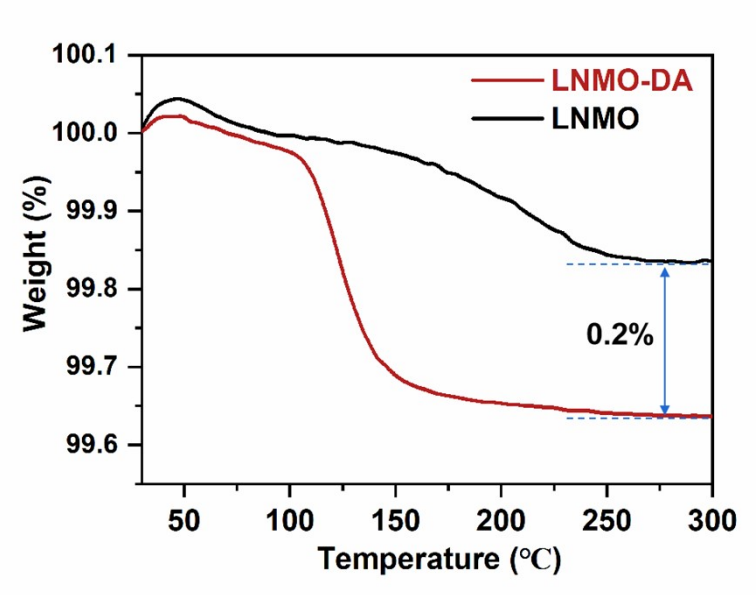

Fig. S2 Thermogravimetric curves of LNMO and LNMO-DA materials.

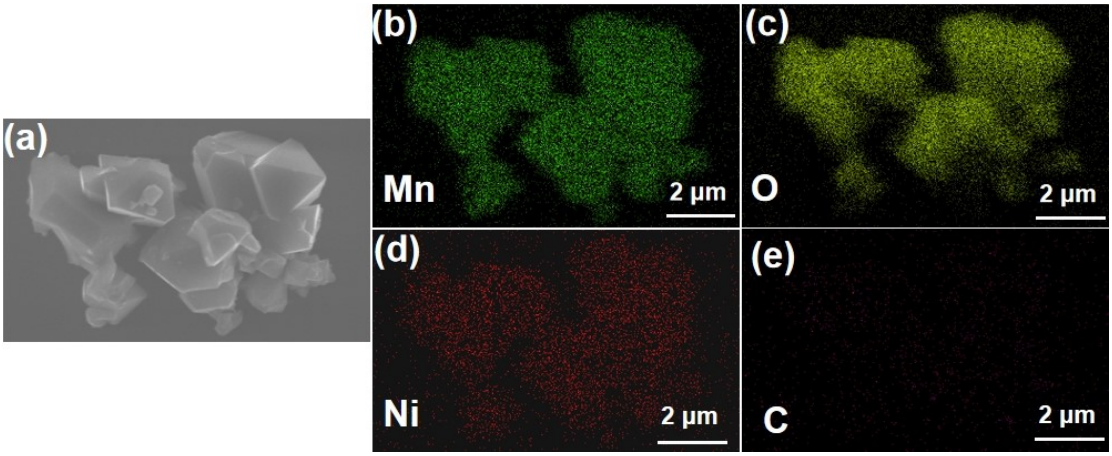

Fig. S3 Elemental mapping of LNMO showing the homogeneous distribution of Mn, Ni,O,and C elements.

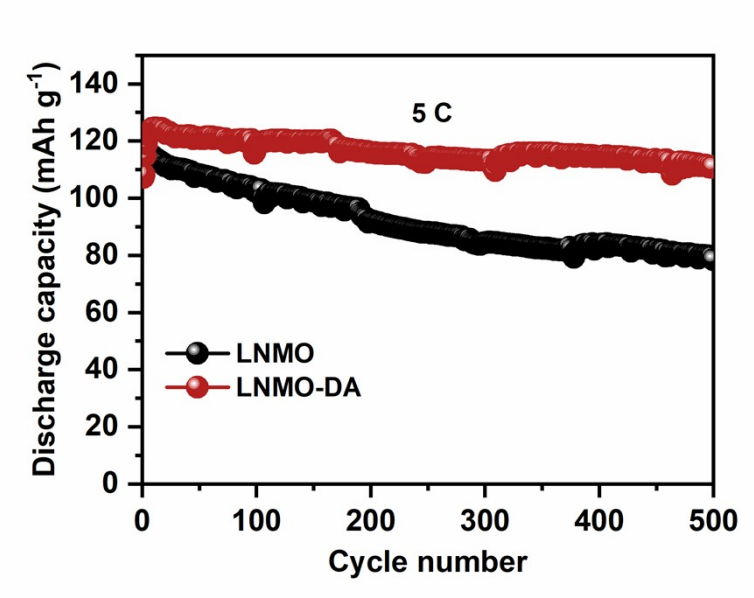

Fig. S4 Rate performance of LNMO and LNMO-DA at 5 C.

The specific proportion of pseudo-capacitance behavior contribution is evaluated by the following formula[1]:

$$i(v) = k1v + k2v^{1/2}$$

where $k1v$ and $k2v^{1/2}$ represent the contributions of the pseudo-capacitance process and the diffusion process, respectively. Significantly, LNMO-DA demonstrates an elevated ratio of pseudo-capacitance, stemming from the electrode surface's concentration of reaction sites. Relative to LNMO, LNMO-DA's pseudo-capacitive lithium retention mechanism inflicts less structural degradation. This approach enhances the material's cycling stability and boosts the efficiency of charge/discharge cycles, particularly under high current conditions as depicted in Fig. S4. This pseudo-capacitance mechanism in LNMO-DA expedites carrier transport, ensuring superior rate capability and prolonged cycling life, alongside structural integrity.

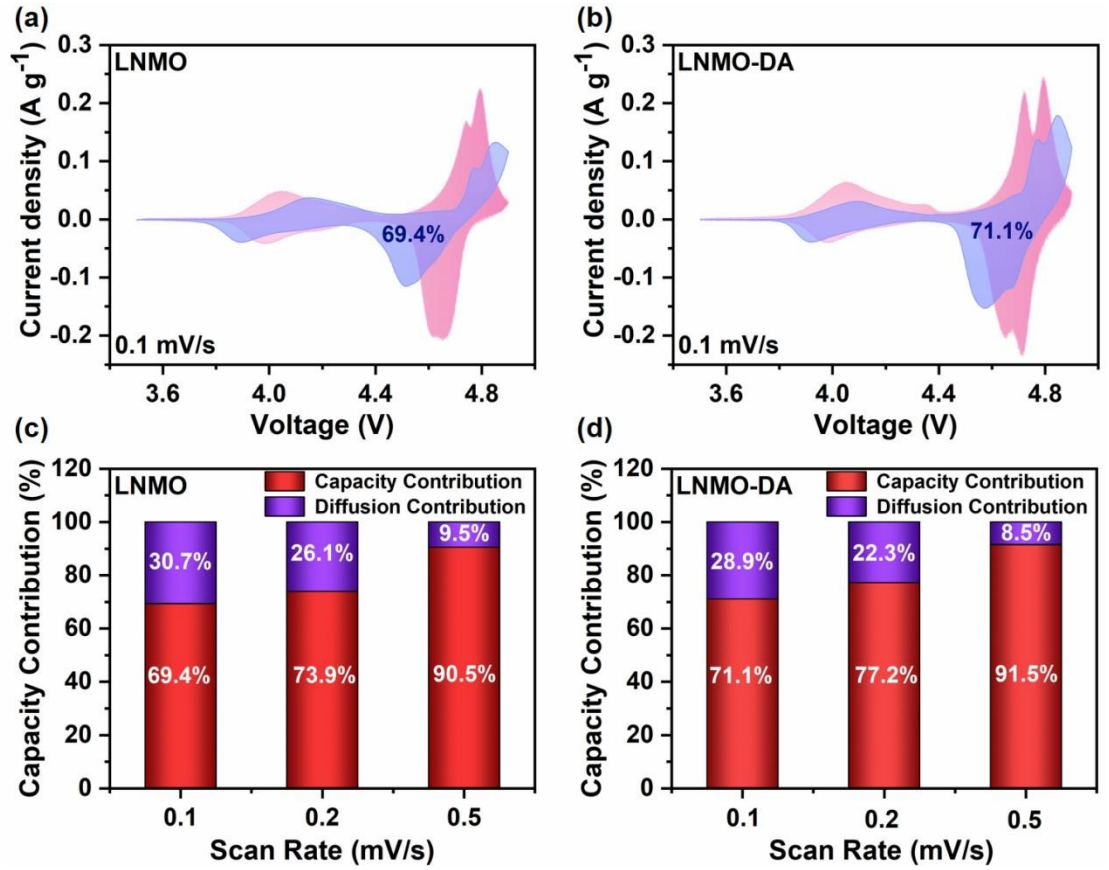

Fig. S5 Capacitive contribution at 0.1 mV s^{-1} of (a) LNMO and (b) LNMO-DA. Contribution proportions of capacitive behavior and diffusion for (a) LNMO and (b) LNMO-DA at different scan rates.

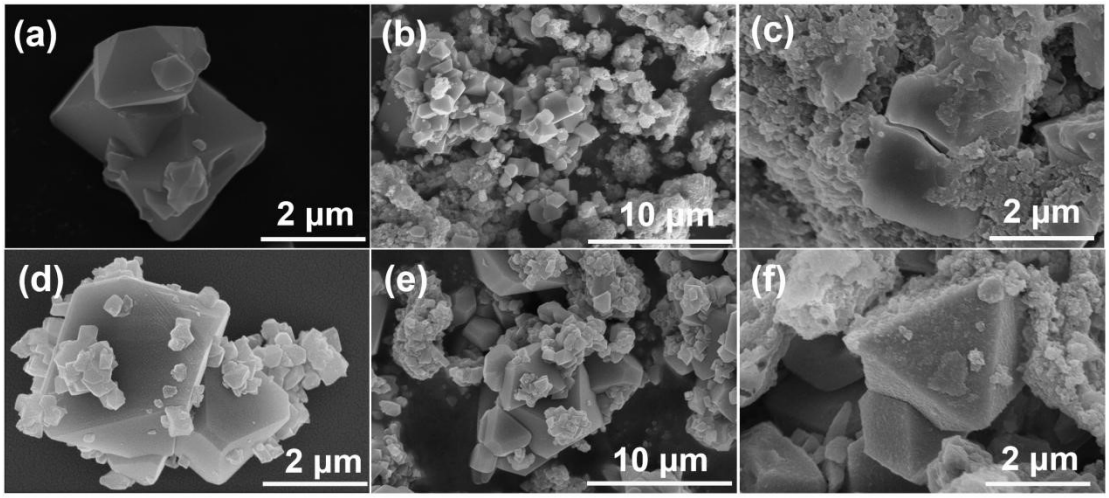

Fig. S6 SEM images of (a,b) LNMO and (d,e) LNMO-DA before cycling. SEM images with low magnification of (c) LNMO and (f) LNMO-DA after cycling.

1. *X. Xu, Q. Liu, H. Zhu, S. Cao and Y. Liu, ACS Sustainable Chem. Eng., 2023,* ***11****,* 15006–15019.